

# Corrosion behavior of steel in pore solutions extracted from different blended cements

Miha Hren | Tadeja Kosec  | Andraž Legat

Dedicated to Professor Dr-Ing. Michael Raupach on the occasion of his 60<sup>th</sup> birthday

Slovenian National Building and Civil Engineering Institute, Laboratory for metals, corrosion and anticorrosion protection, Ljubljana, Slovenia

## Correspondence

Tadeja Kosec, Slovenian National Building and Civil Engineering Institute, Dimičeva 12, 1000 Ljubljana, Slovenia.  
Email: [tadeja.kosec@zag.si](mailto:tadeja.kosec@zag.si)

## Funding information

Slovenian Research Agency

## Abstract

Mortar specimens made from four different types of cement, CEM I, CEM II, CEM III, and CEM IV, were prepared and pore solutions extracted. Three different types of exposure were studied: noncarbonated without chlorides, noncarbonated with chlorides, and carbonated with chlorides. Various electrochemical methods (linear polarization, potentiodynamic polarization measurements) were implemented to characterize the processes of corrosion on steel in these solutions. The type and extent of corrosion products were evaluated by means of various spectroscopic techniques. Specific differences in the type and extent of corrosion damage were determined and compared for each of the extracted pore solutions from the different blended cements. An attempt was made to classify these differences in comparison with the reference cement (CEM I) and in relation to the different types of exposure.

## KEYWORDS

electrochemical properties, pore water, Raman analysis, steel

## 1 | INTRODUCTION

Corrosion of steel is one of the main reasons for reduced service life of reinforced concrete structures.<sup>[1,2]</sup> In the last four decades, considerable advancements have been made toward better understanding the mechanisms of steel corrosion in concrete environments.<sup>[1–6]</sup> The main two mechanisms which cause corrosion of steel in concrete are the ingress of halide ions (mainly chlorides from deicing salts and chlorides in the atmosphere close to marine environments), and carbonation, which lowers the pH environment in concrete.<sup>[3]</sup>

In blended cements, the use of mineral admixtures influences the processes of corrosion and propagation by refining concrete pores that can slow down chloride penetration and carbonation.<sup>[7,8]</sup> The same reactions that

refine the pores also reduce alkalinity<sup>[9]</sup> and affect chloride binding,<sup>[10]</sup> thus creating a different and unknown corrosive environment. Several studies have investigated the impact of different blended cements on cements' material properties.<sup>[11–13]</sup>

Various experiments in pore water have been carried out to explain the differences in corrosion behavior of steel in specific blended cements.<sup>[14–22]</sup> Most of them have been conducted using simulated pore solutions,<sup>[14,15,18,20,21]</sup> with the number of measurements in extracted pore solutions being fairly low.<sup>[22]</sup>

Simulated pore water solutions used in the studies usually consisted of saturated calcium hydroxide, with potassium and sodium hydroxide added to achieve the high pH values required.<sup>[20]</sup> The pH of such solutions might vary upon exposure to air, as a reduction in pH is

This is an open access article under the terms of the Creative Commons Attribution License, which permits use, distribution and reproduction in any medium, provided the original work is properly cited.

© 2020 The Authors. *Materials and Corrosion* published by Wiley-VCH Verlag GmbH & Co. KGaA

observed due to a reaction with  $\text{CO}_2$ .<sup>[20]</sup> In some cases, therefore, the corrosion properties of steel in simulated concrete pore waters made of saturated calcium hydroxide were compared with buffers with a stable and defined pH, sometimes with the addition of chlorides.<sup>[21]</sup>

As already highlighted, there are far fewer corrosion studies available considering concrete pore solutions extracted from blended cements. Newly developed blended cements exhibit different properties and the behavior of steel in these cements is thus still under investigation.

The aim of the present paper is to study the corrosion behavior of steel in simulated concrete pore waters from mortars prepared using CEM I, CEM II, CEM III, and CEM IV cements. Three types of environment were studied: mortars without carbonation and without chlorides, mortars without carbonation exposed to cyclic wetting with chlorides, and mortars exposed to accelerated carbonation and cyclic wetting with chlorides. Pore waters were extracted from mortar specimens and subsequently analyzed. Simulated pore water solutions were then prepared. Different electrochemical techniques (open-circuit potential [OCP] measurements, linear polarization, and potentiodynamic measurements) were used to study the corrosion properties of steel in different corrosive environments. After exposure to different environments, the steel surfaces were optically and spectroscopically examined.

## 2 | MATERIALS AND METHODS

### 2.1 | Simulated pore solutions from mortars

Multiple mortar prisms  $100 \times 60 \times 30$  mm in size were prepared. Each prism had a water–cement ratio of 0.75 and a cement–aggregate ratio of 0.33. Standard sand as described in EN 196-1:2016 was used and mixed with one of four different cements, namely CEM I, CEM II, CEM III, and CEM IV. The composition of the cements varied with respect to the content of CaO,  $\text{SiO}_2$ , Cl,  $\text{Al}_2\text{O}_3$ , and so forth, the type and composition of each cement are shown in Table 1. All mortar specimens were cured for 28 days in a humidity chamber. One set of mortar specimens further underwent accelerated carbonation for a period of 10 weeks. Chlorides were added through cyclic ponding of a 3.5% sodium chloride solution,

using a 7-day cycle consisting of 3 days of wetting followed by 4 days of drying. Reference specimens of each cement type were also made to obtain pore water of uncarbonated mortars without chlorides.

After 35 weeks of chloride exposure, pore solutions were extracted from the specimens using the technique described by Cyr et al.<sup>[23]</sup> The solution was drained through a filter using a special device that exerts compressive pressure on the specimen in the range of 500 to 1,000 MPa. A few milliliters of the solution was extracted, diluted, and analyzed using chromatography. Based on these results, a total of 12 synthetic pore solutions were prepared, varying by cement type, chloride content, and carbonation state. Table 2 shows the synthetic pore solutions prepared for electrochemical tests.

### 2.2 | Electrochemical measurements

One millimeter steel sheets were cut into discs and used as working electrodes for electrochemical testing. They were abraded with 1,000-grit emery paper and cleaned in ethanol solution for 3 min using an ultrasonic bath.

Electrochemical measurements were performed in synthetic pore water solutions (Table 2). The pH value used is stated in the table.

A three-electrode corrosion cell was used, with a volume of  $350 \text{ cm}^3$ . The working electrode had an exposed surface area of  $0.785 \text{ cm}^2$ . A Gamry 600 potentiostat/galvanostat, expanded with a Gamry Instruments framework module, was used for the electrochemical tests. All potentials are reported with respect to the saturated calomel electrode (SCE) scale.

The electrochemical tests consisted of a minimum 22-hr stabilization period at OCP, followed by linear polarization measurement at a scan rate of  $0.1 \text{ mV/s}$  around  $\pm 20 \text{ mV}$  versus OCP. Potentiodynamic measurements were then run from  $-0.25 \text{ V}$  versus OCP on the cathodic side, and from OCP to  $+0.80 \text{ V}$  on the anodic side, at a scan rate of  $1 \text{ mV/s}$ .

### 2.3 | Surface characterization and spectroscopic analysis

To assess the corrosion damage and determine the type of corrosion products, steel sheet specimens were immersed in

Cement	CaO	$\text{SiO}_2$	$\text{Al}_2\text{O}_3$	$\text{Fe}_2\text{O}_3$	MgO	Cl	$\text{SO}_3$	$\text{Na}_2\text{O}$	$\text{K}_2\text{O}$
CEM I 42.5N	63.37	19.57	4.43	2.95	1.63	0.057	2.91	0.28	0.76
CEM II/B-M (LL-V) 42.5N	54.97	20.51	5.5	3.16	1.84	0.047	2.57	0.3	0.79
CEM III/B 32,5N-LH/SR	45.38	30.75	7.87	1.71	6.16	0.142	2.25	0.3	0.59
CEM IV/A (V-P) 42,5R SR	49.38	27.36	7.93	3.93	1.8	0.038	2.59	0.51	1.02

**TABLE 1** Chemical composition of cements investigated, by percentage

**TABLE 2** pH, chloride concentration, and  $[\text{Cl}^-]/[\text{OH}^-]$  ratio in tested pore solutions (g/L)

Noncarbonated without chloride				Noncarbonated with chlorides				Carbonated with chlorides			
Pore solution	pH	$\text{Cl}^-$	$[\text{Cl}^-]/[\text{OH}^-]$	Pore solution	pH	$\text{Cl}^-$	$[\text{Cl}^-]/[\text{OH}^-]$	Pore solution	pH	$\text{Cl}^-$	$[\text{Cl}^-]/[\text{OH}^-]$
CEM I	13.06	0.07	0.017	CEM I	12.05	61.04	153	CEM I	10.45	82.8	$8.29 \times 10^3$
CEM II	13.03	0.10	0.026	CEM II	11.81	84.86	371	CEM II	7.52	106	$9.06 \times 10^6$
CEM III	12.51	0.40	0.349	CEM III	11.45	47.99	480	CEM III	7.54	117	$9.53 \times 10^6$
CEM IV	13.01	0.06	0.017	CEM IV	12.06	74.91	184	CEM IV	9.83	110	$4.59 \times 10^4$

each of the 12 synthetic pore solutions for a period of 18 days. Following exposure, the surface morphology was inspected and analyzed with a low vacuum scanning electron microscope (SEM; JSM 5500 LV; JOEL, Japan) at an acceleration voltage of 20 kV.

Raman spectra were also obtained using a Horiba Jobin Yvon LabRAM HR800 Raman spectrometer coupled to an Olympus BXM optical microscope. The measurements were performed using a 633-nm laser excitation line, a  $\times 100$  objective lens, and a 600 grooves/mm grating, which gave a spectral resolution of  $2 \text{ cm}^{-1}/\text{pixel}$ . The power of the laser was set to 0.14 mW. A multichannel air-cooled charge-coupled device detector was used, with integration times of between 20 and 30 s. The spectra presented are without baseline correction.

### 3 | RESULTS AND DISCUSSION

The properties of steel in different simulated pore solutions were first studied electrochemically, then, the steel surface and corrosion products underwent spectroscopic investigation.

#### 3.1 | Differences between pore solutions and OCP measurements

The corrosion properties of steel were studied in different pore water solutions, extracted from varying mortar specimens. The composition of these solutions is given in Table 2. It can be observed that the pH values of pore solutions extracted from noncarbonated mortar prisms without chlorides are around pH 13, with the pore solution from the CEM III cement exhibiting the lowest value of 12.51. The  $[\text{Cl}^-]/[\text{OH}^-]$  ratio for noncarbonated specimens without chlorides is low for all studied cements.

In pore solutions extracted from noncarbonated mortars that were cyclically wetted with chlorides, the pH values decreased. The values were slightly lower for pore waters from CEM II and CEM III (11.8 and 11.4, respectively). The  $[\text{Cl}^-]/[\text{OH}^-]$  ratio is higher than that of pore solutions from noncarbonated mortars without chlorides.

In the pore waters extracted from carbonated mortars that were cyclically wetted with NaCl solution, pH values drastically dropped to around 7.5 for CEM II and CEM III, while pH values for CEM I and CEM IV were around 10. The  $[\text{Cl}^-]/[\text{OH}^-]$  ratio is the highest of all pore solutions (Table 2).

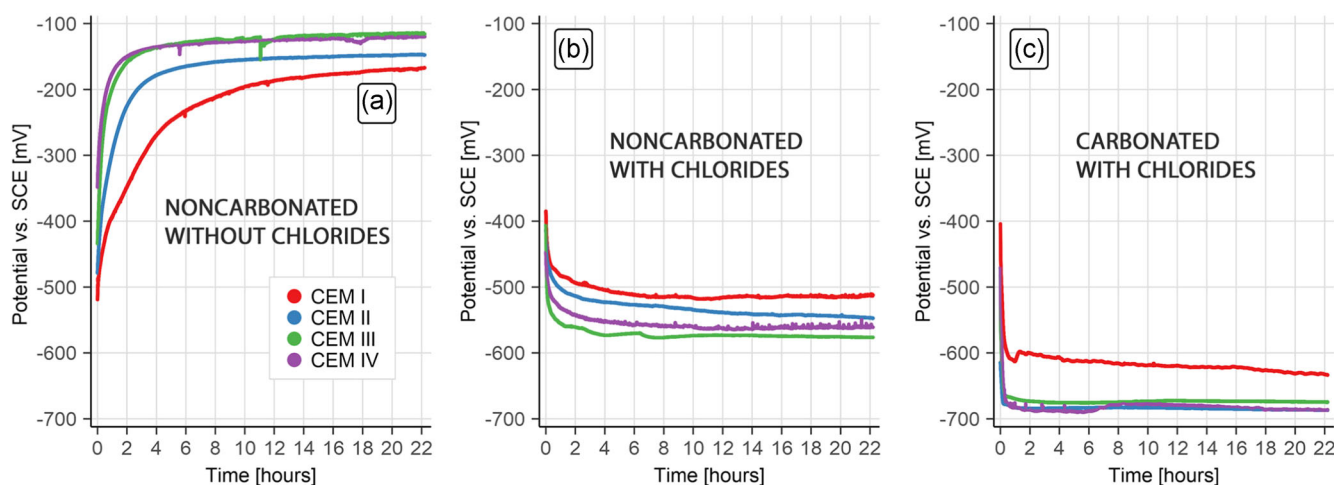


**FIGURE 1**  $E_{\text{corr}}$  for steel in concrete pore solution extracted from mortars with CEM I, CEM II, CEM III, and CEM IV cements: (a) noncarbonated without chlorides, (b) noncarbonated with chlorides, and (c) carbonated with chlorides. SCE, saturated calomel electrode [Color figure can be viewed at [wileyonlinelibrary.com](http://wileyonlinelibrary.com)]

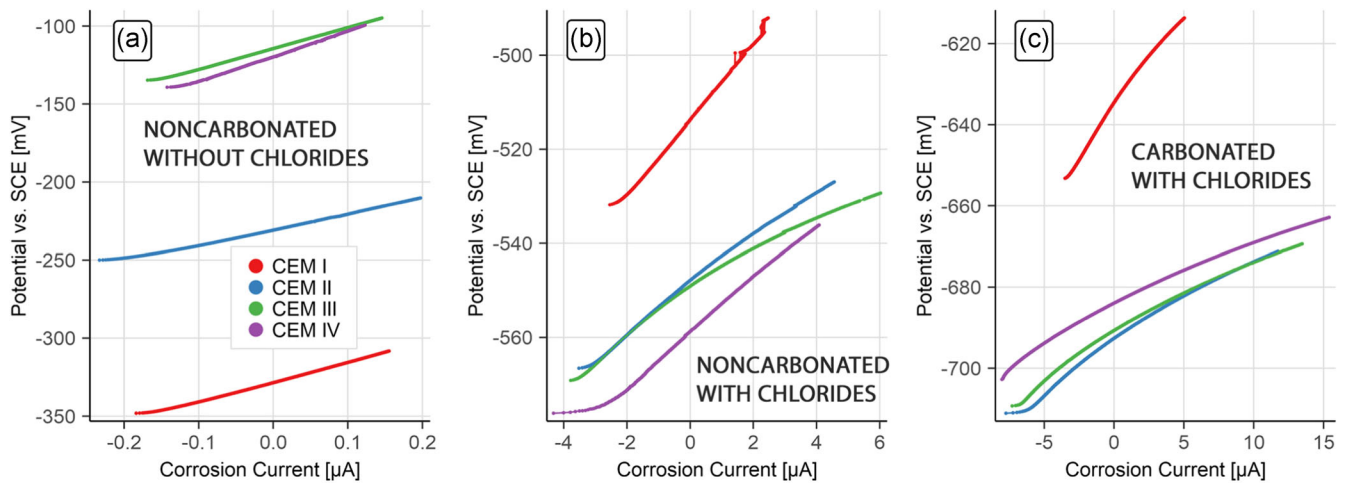


**FIGURE 2** Polarization resistance measurements at a scan rate of 0.1 mV/s for steel in concrete pore solution extracted from mortars with CEM I, CEM II, CEM III, and CEM IV cements: (a) noncarbonated without chlorides, (b) noncarbonated with chlorides, and (c) carbonated with chlorides. SCE, saturated calomel electrode [Color figure can be viewed at [wileyonlinelibrary.com](https://onlinelibrary.wiley.com/doi/10.1002/maco.202011548)]

OCP was measured for more than 20 hr until steady state was reached. The results of OCP measurements are presented in Figure 1. In the noncarbonated pore water solutions without chlorides, OCP values for steels in different cements (CEM I, CEM II, CEM III, and CEM IV) were similar, around  $-150$  mV versus SCE. The potential of the steel shows that steel is passivated in these conditions, as it is relatively positive. In all cases, OCP values increase due to the buildup of a stable passive layer on the steel.<sup>[24]</sup>

It can be observed from Figure 1b that the OCP value in all pore solutions extracted from noncarbonated mortars that were cyclically wetted with chlorides decreased drastically over time. The OCP value was at around  $-560$  mV versus SCE. The decrease in OCP indicated that the passive layer on steel in such pore solutions was obstructed. The potential decrease was most intense in pore water from CEM III.

In carbonated pore solutions with chlorides, it can be observed that OCP values for steel in the different cements (CEM I, CEM II, CEM III, and CEM IV) decreased even more, to a value around  $-700$  mV versus SCE (Figure 1c). Only the OCP value for the CEM I solution showed a smaller decrease, to around  $-620$  mV versus SCE. The steel surface completely depassivated in these conditions.

### 3.2 | Polarization resistance measurements

The polarization resistance for steel samples was measured in different simulated pore solutions following a minimum 22-h stabilization period until OCP was achieved. Results are presented in Figure 2 and Table 3.

In noncarbonated pore solutions without chlorides, it can be observed that polarization resistance values  $R_p$  for steels in the different cements (CEM I, CEM II, CEM III, and CEM IV) were relatively high, at around  $150 \text{ k}\Omega\text{-cm}^2$ . The lowest  $R_p$  was measured in pore water extracted from mortar made with CEM III cement ( $101 \text{ k}\Omega\text{-cm}^2$ ). The results show that steel was passivated in these conditions where a relatively high pH is maintained. The lower  $R_p$  value of steel in pore water from CEM III is related to a lower pH value and a higher  $[\text{Cl}^-]/[\text{OH}^-]$  ratio of the solution (Table 2). In CEM III, a higher concentration of  $\text{Cl}^-$  was also seen (Table 2).

In Figure 2b and Table 3, it can be seen that in pore solutions extracted from noncarbonated mortars that were cyclically wetted with chlorides, the  $R_p$  values decreased

**TABLE 3** Linear polarization resistance measurements,  $R_p$  in  $\text{k}\Omega\text{-cm}^2$

Cement	Noncarbonated, no $\text{Cl}^-$	Noncarbonated with $\text{Cl}^-$	Carbonated with $\text{Cl}^-$
CEM I	$165 \pm 65$	$101 \pm 3.9$	$4.88 \pm 0.32$
CEM II	$154 \pm 58$	$11.4 \pm 6.5$	$2.57 \pm 0.66$
CEM III	$101 \pm 18$	$10.9 \pm 6.1$	$2.33 \pm 0.62$
CEM IV	$170 \pm 42$	$8.9 \pm 3.2$	$2.88 \pm 0.65$

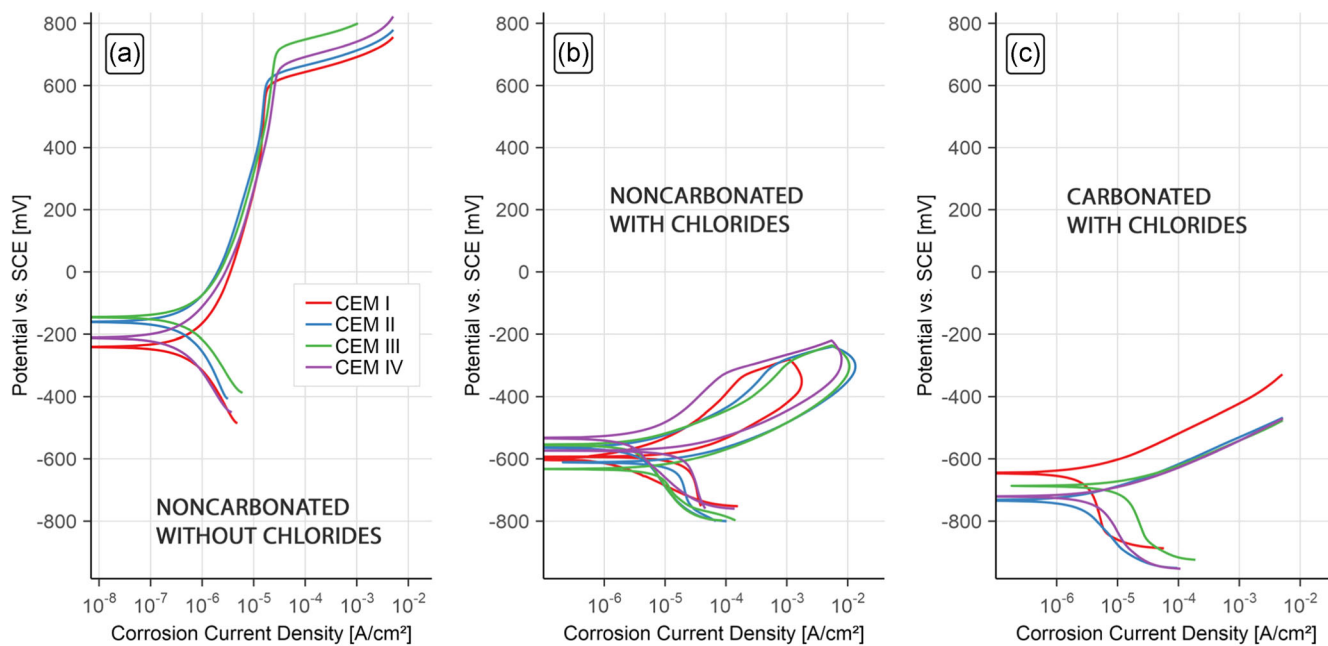


**FIGURE 3** Potentiodynamic measurements for steel at a scan rate of 1 mV/s in concrete pore solutions extracted from mortars with cement types CEM I, CEM II, CEM III, and CEM IV: (a) noncarbonated without chlorides, (b) noncarbonated with chlorides, and (c) carbonated with chlorides. SCE, saturated calomel electrode [Color figure can be viewed at [wileyonlinelibrary.com](https://onlinelibrary.wiley.com/doi/10.1002/maco.202011548)]

drastically in all solutions except in CEM I.  $R_p$  values were 10 times lower for CEM II, CEM III, and CEM IV pore solutions at around  $10 \text{ k}\Omega\text{-cm}^2$ , while only a 1.6-time decrease of  $R_p$  value was observed for CEM I solution. In the case of the latter, the  $[\text{Cl}^-]/[\text{OH}^-]$  ratio was also the lowest when compared with other pore waters, which had an effect on the polarization resistance value of steel.

In carbonated pore water solutions with chlorides, it can be observed that  $R_p$  values for steel in cement types CEM II, CEM III, and CEM IV were about 40 to 60 times lower when compared with pore waters without chlorides.  $R_p$  values for the CEM I solution were about 34-times smaller. In this case, the  $[\text{Cl}^-]/[\text{OH}^-]$  ratio for CEM I was the lowest of all cement types. In these conditions, the steel was in a depassivated state.

### 3.3 | Potentiodynamic experiments

After polarization resistance measurements, potentiodynamic scans over a wide potential region were carried out. Representative curves for each cement type are presented in Figure 3.

It can be observed that all potentiodynamic scans are similar in noncarbonated pore waters without chlorides. Corrosion current densities, corrosion potentials, and breakdown potentials  $E_b$  are also similar (Figure 3a). A passive region is indicated by the curves with a breakdown potential of around 700 mV versus SCE.

In noncarbonated mortars that were cyclically wetted with chlorides, cyclic potentiodynamic curves exhibited positive hysteresis, showing a possible occurrence of localized

**TABLE 4** Corrosion rates in  $\mu\text{m}/\text{year}$

Cement type	Noncarbonated, no $\text{Cl}^-$		Noncarbonated with $\text{Cl}^-$		Carbonated with $\text{Cl}^-$	
	$R_p$	PD scans*	$R_p$	PD scans	$R_p$	PD scans
CEM I	7.7	5.7	75.1	22.8	94	57.0
CEM II	10.4	8.0	43.8	45.6	139	45.6
CEM III	19.2	8.0	42.0	57.0	146	228
CEM IV	8.1	5.7	53.3	57.0	136	68.4

\*PD scans- results obtained from potentiodynamic curves.

corrosion. Corrosion potential lowered to a value of around  $-600$  mV and corrosion current density values were lower compared with pore water without chlorides (Figure 3b).

In carbonated pore solutions with chlorides, potentiodynamic curves show that the steel is depassivated in all solutions, as the current density measured in the anodic part of the curve increases more rapidly (Figure 3c). No passive

region is observed, corrosion potential decreased even more, and corrosion current densities were high compared with previous states. No differences in electrochemical behavior between different pore solutions were observed. General corrosion over the examined surface was observed.

Corrosion rates ( $\mu\text{m}/\text{year}$ ) were also roughly estimated from  $R_p$  values, which are shown in Table 3. Corrosion

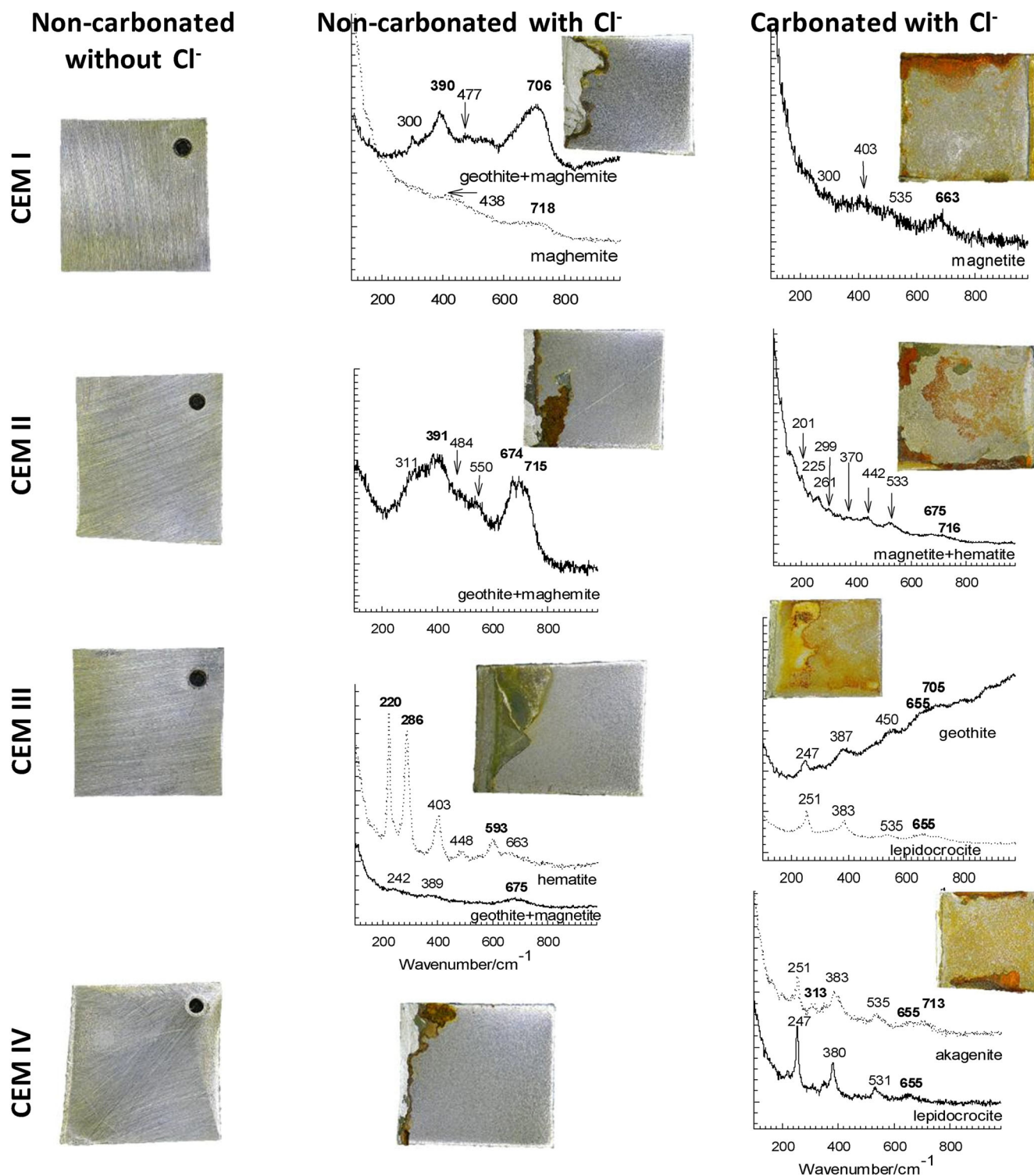


**FIGURE 4** Images of the samples immersed in pore water solutions for 18 days. Raman spectra were obtained on corrosion products. Images with no spectra showed no Raman activity [Color figure can be viewed at [wileyonlinelibrary.com](http://wileyonlinelibrary.com)]

current densities were approximately assessed from the potentiodynamic scans in Figure 3 and thereafter transferred into the corrosion rates. Both estimated groups of the corrosion rates are shown in Table 4. It was clear that the lowest corrosion rates were observed in pore solutions from noncarbonated mortars without chlorides. Significant differences were also observed between pore solutions from carbonated and noncarbonated mortars with chlorides. A higher corrosion rate was found in the pore solution from the carbonated CEM III mortar with chlorides, but differences between other mortars were minor. It should be emphasized, however, that the actual surface of corrosion areas is unknown, and thus localization of corrosion could play a significant role in this estimation.

### 3.4 | Spectroscopic investigation of the analyzed steel surfaces

Figure 4 shows steel surfaces after 18 days of immersion in the different pore solutions. All specimens exposed for 18 days to solutions from the noncarbonated mortars without chlorides remained passive and no corrosion products were found. Raman spectra were obtained for the corrosion products developed in pore waters extracted from noncarbonated mortars with chlorides and carbonated mortars with chlorides. Images that show no Raman spectra had no visible corrosion products, especially in pore waters that were extracted from mortars without cyclic chloride exposure and without carbonation. On some samples, corrosion products did not show on Raman spectra or were hard to distinguish from deposited salts and mortar.

Goethite and maghemite were found on the steel sample exposed to noncarbonated pore water with chlorides, extracted from CEM I mortar. The most intensive bands of goethite ( $\alpha$ -FeOOH) were expressed at 300, 390, 477, 547, and 682  $\text{cm}^{-1}$ , while the most intensive broad bands of maghemite ( $\gamma$ -Fe<sub>2</sub>O<sub>3</sub>) were seen at 346, 500, and 718  $\text{cm}^{-1}$ .

Goethite and maghemite, that is, a mixture of  $\alpha$ -FeOOH and  $\gamma$ -Fe<sub>2</sub>O<sub>3</sub>,<sup>[25]</sup> were also found on the steel surface exposed to simulated pore water extracted from noncarbonated CEM II mortar, with the most intensive bands occurring at 311, 391, 484, 550, 674, and 715  $\text{cm}^{-1}$ .

After 18 days of exposure to pore water extracted from noncarbonated CEM III water with chlorides, goethite with magnetite and hematite were found on the steel surface. Raman spectra showed broad bands of magnetite (Fe<sub>3</sub>O<sub>4</sub>) at 300, 403, 535, and 663  $\text{cm}^{-1}$ , while the most intensive band of goethite was observed at 242, 387, and 682  $\text{cm}^{-1}$ . Hematite ( $\alpha$ -Fe<sub>2</sub>O<sub>3</sub>) was also found, with bands observed at 220,

245 (as a shoulder), 286, and 403  $\text{cm}^{-1}$ , and less intensive bands at 593 and 663  $\text{cm}^{-1}$ . Corrosion products on the steel immersed in pore water extracted from noncarbonated CEM IV water with chlorides showed no Raman activity.

Steel samples exposed to extracted carbonated pore water with chlorides were more heavily corroded, as seen from the images in Figure 4.

Magnetite was found on the steel sample immersed in carbonated pore water from CEM I mortar with chlorides. On the steel sample immersed in carbonated pore water from CEM II mortar with chlorides, Raman investigation revealed the presence of magnetite and hematite. Goethite and lepidocrocite were found on the steel surface exposed to pore water from CEM III mortar, while akaganeite and lepidocrocite were observed on the surface of the steel exposed to CEM IV pore water. Raman spectra detected bands of lepidocrocite ( $\gamma$ -FeOOH) at 251, 383, 535, and 655  $\text{cm}^{-1}$ . Lepidocrocite has been found to be unstable and porous,<sup>[17]</sup> and tends to dissolve and transform into other forms of oxide over time, thus offering weaker corrosion protection. Raman spectra for akaganeite ( $\beta$ -FeOOH) showed bands at 251, 313, 383, 535, 655, and 713  $\text{cm}^{-1}$ .

## 4 | CONCLUSIONS

Steel corrosion was studied in simulated concrete pore waters extracted from mortars made from CEM I and different blended cements (CEM II, CEM III, and CEM IV). Three different types of exposure were studied: (a) no carbonation and no addition of chlorides, (b) a noncarbonated environment with chlorides, and (c) a carbonated environment with chlorides. Various electrochemical tests were conducted in different simulated concrete pore waters and spectroscopic investigation was carried out after exposure of steel to the tested environments. The following conclusions were drawn:

- Carbonation of the mortars greatly affected the pH value of extracted pore solutions. The pH value decreased even more if the samples were cyclically wet with a NaCl solution. The decrease in pH value due to carbonation was higher in the case of CEM II and CEM III cements.
- Certain differences in the Cl<sup>-</sup> content of pore water solutions from mortars made from CEM I, CEM II, CEM III, and CEM IV cements were found, but they were not significant. Generally, the differences were bigger for carbonated mortars. In the case of noncarbonated mortars, the Cl<sup>-</sup> content was highest in CEM II, whereas in the case of carbonated mortars the Cl<sup>-</sup> content was highest in CEM III.

- Large differences in pH values had a significant influence on the  $[Cl^-]/[OH^-]$  ratios. For carbonated mortars, the  $[Cl^-]/[OH^-]$  ratios were between two and four orders of magnitude higher than for noncarbonated mortars. The lowest was for CEM I, whereas the highest was for CEM III and CEM II.
- Electrochemical investigation showed that OCP values decreased when chlorides were present, and that they decreased even more when specimens were also carbonated. The polarization resistance of steel in simulated pore water solutions also decreased when mortars were cyclically wet with chlorides, and even more so when carbonated.
- Potentiodynamic measurements in noncarbonated pore waters from different blended mortars without chlorides exhibited a passive region in the anodic part of the curve, showing a passive state of steel in such environments. A tendency toward local steel corrosion was demonstrated in noncarbonated specimens with chlorides, where an increase in corrosion current density was also observed. In the carbonated environment with chlorides, potentiodynamic curves showed that the steel underwent active corrosion of the general type.
- According to the shapes of potentiodynamic scans and the types of corrosion damage, it can be assumed that the main differences in measured electrochemical parameters ( $R_p$ ,  $j_{corr}$ ) and corrosion rates ( $v_{corr}$ ) emerged from different surface areas of active corrosion.
- Optical observation and Raman analysis on corroded steel specimens in noncarbonated environments with chlorides showed local attack with the presence of maghemite and goethite, which were also observed in CEM III pore water. In carbonated environments with chlorides, general corrosion attack was observed, while spectral analysis showed the presence of magnetite, hematite, goethite, and akaganeite, as well as unstable and porous lepidocrocite. It could be concluded that maghemite and goethite provided a fairly stable protective layer, whereas hematite and lepidocrocite are not stable corrosion products.

#### ACKNOWLEDGMENT

This study was performed under Slovenian research agency (SRA) funding within the Young Scientist programme of Miha Hren.

#### DATA AVAILABILITY STATEMENT

The raw/processed data required to reproduce these findings cannot be shared at this time as the data also forms part of an ongoing study.

#### ORCID

Tadeja Kosec  <http://orcid.org/0000-0001-6790-1880>

#### REFERENCES

- [1] B. B. Hope, C. L. Page, *Cem. Concr. Res.* **1986**, *16*, 771.
- [2] L. Bertolini, B. Elsener, P. Pedferri, R. Polder, *Corrosion of Steel in Concrete: Prevention, Diagnosis, Repair*, Wiley-VCH, Weinheim **2004**.
- [3] G. K. Glass, C. L. Page, N. R. Short, *Corros. Sci.* **1991**, *32*, 1283.
- [4] R. B. Polder, W. H. A. Peelen, *Cem. Concr. Compos.* **2002**, *24*, 427.
- [5] M. Raupach, *Constr. Build. Mater.* **1996**, *10*, 329.
- [6] M. Raupach, P. Schießl, *NDT&E Int.* **2001**, *34*, 435.
- [7] P. K. Mehta, P. J. M. Monteiro, *Concrete: Microstructure, Properties, and Materials*, McGraw-Hill, New York, NY **2006**.
- [8] J. Bijen, *Constr. Build. Mater.* **1996**, *10*, 309.
- [9] A. Vollpracht, B. Lothenbach, R. Snellings, J. Haufe, *Mater. Struct.* **2016**, *49*, 3341.
- [10] Q. Yuan, C. Shi, G. De Schutter, K. Audenaert, D. Deng, *Constr. Build. Mater.* **2009**, *23*, 1.
- [11] M. A. Ibrahim, A. E.-D. M. Sharkawi, M. M. El-Attar, O. A. Hodhod, *Constr. Build. Mater.* **2018**, *168*, 21.
- [12] E. Güneş, T. Özturan, M. Gesoğlu, *Cem. Concr. Compos.* **2005**, *27*, 449.
- [13] O. S. B. Al-Amoudi, *Build. Environ.* **1998**, *33*, 53.
- [14] R. Liu, L. Jiang, J. Xu, C. Xiong, Z. Song, *Constr. Build. Mater.* **2014**, *56*, 16.
- [15] W. Chen, R.-G. Du, C.-Q. Ye, Y.-F. Zhu, C.-J. Lin, *Electrochim. Acta* **2010**, *55*, 5677.
- [16] A. Poursaeed, C. M. Hansson, *Cem. Concr. Res.* **2007**, *37*, 1127.
- [17] J. K. Singh, D. D. N. Singh, *Corros. Sci.* **2012**, *56*, 129.
- [18] D. Addari, B. Elsener, A. Rossi, *Electrochim. Acta* **2008**, *53*, 8078.
- [19] P. Ghods, O. B. Isgor, G. McRae, T. Miller, *Cem. Concr. Compos.* **2009**, *31*, 2.
- [20] M. Moreno, W. Morris, M. G. Alvarez, G. S. Duffó, *Corros. Sci.* **2004**, *46*, 2681.
- [21] A. Česen, T. Kosec, A. Legat, V. Bokan-Bosiljkov, *Mater. Technol.* **2014**, *48*, 51.
- [22] M. Hren, T. Kosec, A. Legat, V. Bokan-Bosiljkov, *Mater. Technol.* **2019**, *53*, 679.
- [23] M. Cyr, P. Rivard, F. Labrecque, A. Daidié, *J. Am. Ceram. Soc.* **2008**, *91*, 2653.
- [24] W. S. Tait, *An Introduction to Electrochemical Corrosion Testing for Practicing Engineers and Scientists*, Ohio State University, Columbus, OH **1994**.
- [25] F. Dubois, C. Mendibide, T. Pagnier, F. Perrard, C. Durret, *Corros. Sci.* **2008**, *50*, 3401.

**How to cite this article:** Hren M, Kosec T, Legat A. Corrosion behavior of steel in pore solutions extracted from different blended cements. *Materials and Corrosion*. 2020;71:759–766.

<https://doi.org/10.1002/maco.202011548>